ACS Medicinal Chemistry Letters
Cite This: ACS Med. Chem. Lett. 2018, 9, 929−934
Letter
pubs.acs.org/acsmedchemlett

Binding Motifs in the CBP Bromodomain: An Analysis of 20 Crystal Structures of Complexes with Small Molecules

Jian Zhu,[†] Jing Dong,[†] Laurent Batiste,[†] Andrea Unzue,[‡] Aymeric Dolbois,[‡] Vlad Pascanu,[‡] Paweł Śledź,[†] Cristina Nevado,*[,‡] and Amedeo Caflisch*[,†]

[†]Department of Biochemistry, and [‡]Department of Chemistry, University of Zurich, Winterthurerstrasse 190, CH-8057 Zurich, Switzerland

Supporting Information

ABSTRACT: We analyze 20 crystal structures of complexes between the CBP bromodomain and small-molecule ligands that belong to eight different chemotypes identified by docking. The binding motif of the moiety that mimics the natural ligand (acetylated side chain of lysine) at the bottom of the binding pocket is conserved. In stark contrast, the rest of the ligands form different interactions with different side chains and backbone polar groups on the outer rim of the binding pocket. Hydrogen bonds are direct or water-bridged. van der Waals contacts are optimized by rotations of hydrophobic side chains and a slight inward displacement of the ZA loop. Rare types of interactions are observed for some of the ligands.

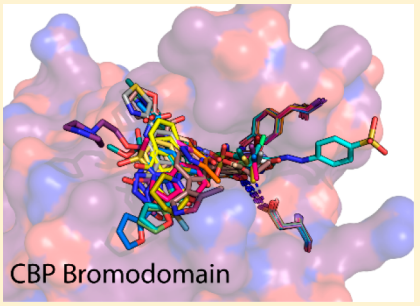

KEYWORDS: *CBP bromodomain, docking, fragment-based ligand design, structure-based hit optimization, cancer*

Bromodomains are protein modules that bind polypeptide segments with acetylated lysine[1] or other acyl modifications of the lysine side chain.[2] Structurally, bromodomains consist of a left-handed four-helix bundle of about 110 residues. The lysine acetyltransferase CBP (CREB binding protein; CREB = cyclic-AMP response element binding protein) is a multidomain protein that regulates transcription. CBP has been studied intensively due to its role in several cellular processes and potential implications in cancer.[3] The single bromodomain of CBP has been shown to recognize histone tails and nonhistone proteins, e.g., p53 acetylated at Lys382 following DNA damage.[4] Small-molecule ligands of the single bromodomain of CBP have been identified by *in vitro* techniques[5−7] and by *in silico* screening using high-throughput fragment docking.[8,9] Optimization by medicinal chemistry into potent and selective CBP bromodomain inhibitors has been reported by others[10] and us.[11,12] The potential applications of drug candidates that target the CBP bromodomain range from castration-resistant prostate cancer[13] to acute myeloid leukemia and cancer immunotherapy.[10]

Here we present an analysis of 20 crystal structures of the CBP bromodomain in complex with small-molecule ligands that originate from *in silico* screening (Table 1). Thirteen of these structures are disclosed for the first time. We focus the analysis on crystal structures solved in the laboratory of the last author because this subset of the ever growing number of available holo structures of the CBP bromodomain is large enough to provide evidence of the heterogeneous interactions.

RESULTS

We use the term headgroup (or simply head) for the part of the ligands that mimics the side chain of the acetylated lysine of the endogenous ligand. The remaining part of the ligand is described as linker and tail group. Despite the variability of head groups there are two conserved hydrogen bonds at the bottom of the acetyl-lysine pocket with two side chains that are present in most of the 61 human bromodomains. These are a direct hydrogen bond with the side chain of Asn1168 and a water-bridged polar interaction with the Tyr1125 (Figure 1A). While in compounds **1**−**19** a single carbonyl oxygen forms both hydrogen bonds, the N3 and N9 atoms of the adenine headgroup of compound **20** are involved in the direct and water-bridged hydrogen bonds (Figure 1B), respectively.

Another conserved interaction in the bottom of the pocket is the optimal packing of a methyl with the side chain of Phe1111. The only two exceptions are the azobenzene derivative **1** which has a chlorine atom next to the phenyl ring of Phe1111 (Figure 1D) and the adenine derivative **20** which has its aromatic C8 atom close to Phe1111.

In stark contrast to the conserved binding motif of the head groups, the tail groups show a large heterogeneity of orientations and interactions (Figures 1A and 2). The intermolecular contacts involve residues of the CBP bromodomain with different flexibility. The side chains of the binding pockets can be grouped into three classes: fully rigid (Pro1106, Pro1110, Phe1111, Val1115, Tyr1125,

Received: June 22, 2018
Accepted: August 8, 2018
Published: August 8, 2018

DOI: 10.1021/acsmedchemlett.8b00286
ACS Med. Chem. Lett. 2018, 9, 929−934

Table 1. 2D Structures and Assay Results of CBP Bromodomain Inhibitors

Cpd	2D Structure	K_D (μM)	IC_{50} (μM)	LE	PDB ID (Res.)[a]	Ref.
1	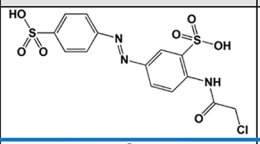	ND	ND	-	5EIC (1.50)	This study
2	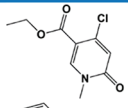	ND	ND	-	5OWK (1.25)	This study
3	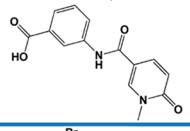	4	ND	0.37	5EP7 (1.20)	This study
4	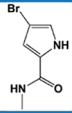	4	40	0.74	5MQE (1.65)	9
5	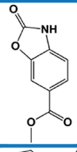	85	455	0.40	5MPZ (1.40)	9
6	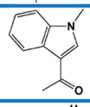	ND	31% @ 0.5M	-	5MQK (1.53)	9
7	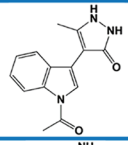	20	ND	0.34	4TS8 (2.00)	21
8	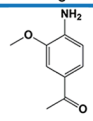	ND	37% @ 0.5M	-	5MQG (1.35)	9
9	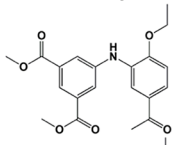	1.4	ND	0.30	5MME (1.35)	This study
10	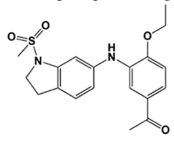	0.970	7.7	0.32	5MMG (1.23)	This study
11	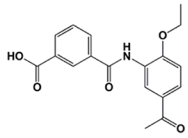	0.770	ND	0.35	4TQN (1.70)	8
12	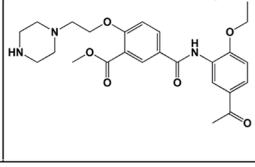	1.4	ND	0.24	5ENG (1.30)	This study
13	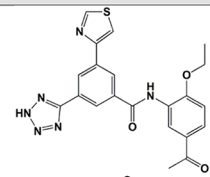	0.003	0.015	0.38	5MPK (1.90)	This study
14	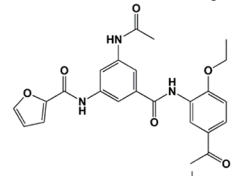	0.035	0.019	0.31	5NLK (1.80)	12
15	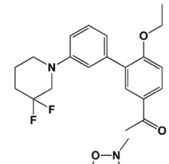	ND	2.2	0.30	6FQU (1.43)	This study
16	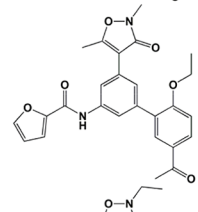	ND	0.140	0.28	6FQO (1.35)	This study
17	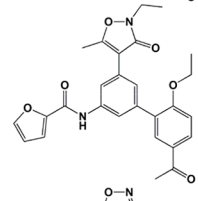	ND	0.146	0.27	6FR0 (1.50)	This study
18	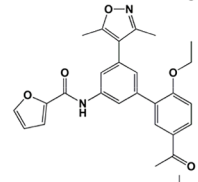	ND	0.040	0.31	6FRF (2.10)	This study
19	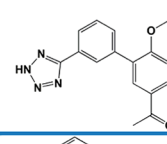	0.085	0.059	0.42	5MPN (1.23)	This study
20	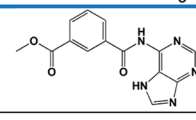	20	ND	0.29	5H85 (1.70)	This study

[a]Diffraction resolutions are reported in angstroms. The head groups of compounds **1** to **20** can be clustered in eight chemotypes (horizontal lines). The 2D structures are oriented with the mimic of the acetylated lysine on the bottom right. The values of the dissociation constant (K_D) were determined in duplicate by the BROMOscan competition binding assay (Figure S5). The IC_{50} values were measured by AlphaScreen (Figure S6).[14] Ligand efficiency[15] is calculated as LE = $-(1.37/HA) \times \log K_D$, in units of kcal/mol per heavy atom (HA). The IC_{50} value is used if the K_D value is not available.

DOI: 10.1021/acsmedchemlett.8b00286
ACS Med. Chem. Lett. 2018, 9, 929−934

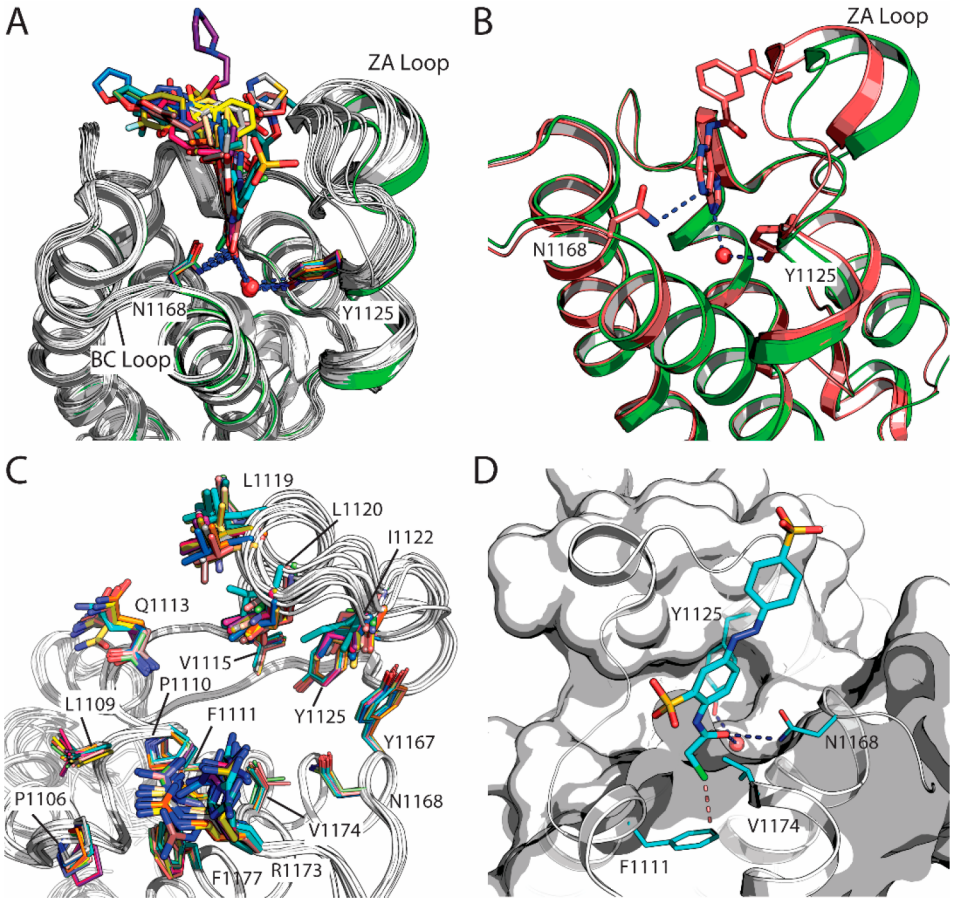

Figure 1. Crystal structures of CBP bromodomain bound to ligands **1**−**20**. The four α-helices of the bromodomain are called Z, A, B, and C, respectively, and the acetyllysine-binding pocket is flanked by two interhelical loops (called ZA and BC loops).[16,17] (A) Structural overlap of the 20 holo structures of the CBP bromodomain (CBP in gray and ligands in different colors) and the apo structure (green). (B) Overlap of the complex with compound **20** (deep salmon) and the apo structure (green). (C) Side chains in the binding site. (D) Structure of CBP (gray) in the complex with the azobenzene derivative **1** (cyan).

Tyr1167, Asn1168, the gatekeeper Val1174, and Phe1177), partially flexible (Leu1120 and Ile1122), and fully flexible (Gln1113, Leu1119, and Arg1173) (Figure 1C). Ligand binding is stabilized by van der Waals interactions with the rigid side chains and the partially flexible Leu1120 and Ile1122. The side chains of Leu1120 and Ile1122 are oriented according to the steric requirements of the different ligands. Furthermore, the ZA loop (residues Arg1103 to Asp1134) adapts to the size of the ligands and shows a slight displacement toward the center of the binding site with respect to the apo structure (Figure 1A).

Concerning the highly flexible side chains, Gln1113 shows two main orientations; it points toward the binding site or completely outside. The inside-orientation of Gln1113 is stabilized by a hydrogen bond with the carbonyl group of Leu1109 as in the apo structure (PDB 3DYW; Figure 2P). Furthermore, there are stacking interactions (e.g., ligands **13**, **14**, and **18**; Figure 2g, 2H and 2L) or hydrogen bonds (e.g., ligands **9**, **10**, **12**, and **14**; Figure 2C, 2D, 2F, and 2H) with the tail group. Gln1113 points outward from the binding site in half of the 20 complexes.

The isoxazol-3-one ring in ligands **16** and **17** and the dimethylisoxazole ring in compound **18** are rotated by about 40 degrees with respect to the phenyl. As a consequence, the methyl next to the oxygen in the ring points downward from the binding site and displaces a water molecule which, in other structures (e.g., apo), is involved in a hydrogen bond to the carbonyl of Pro1114. Thus, it could be beneficial to further modify the isoxazole group to achieve polar interactions with the residues lining the ZA channel, e.g., to form a hydrogen bond with the carbonyl group of Pro1114.

The side chain of Leu1119 is involved in van der Waals contacts with three of the 20 ligands, i.e., **13** (closest distance 4.6 Å), **14** (closest distance 4.4 Å), and one conformation of **18** (closest distance 4.1 Å).

The interaction with the very flexible Arg1173 can be ionic (i.e., salt bridge with the benzoate of compounds **3** and **11** or the tetrazole of **13** and **19**), hydrogen bond-mediated as in compounds **1**, **14**, **16**, **17**, and **18**, charge-dipole as with the $-CF_2-$ of compound **15** (a similar interaction has been reported for an ATAD2 bromodomain ligand),[18] water-bridged (e.g., compound **9**), or absent (compound **20**).

The side chains of Pro1123 and Asp1124 assume a different orientation only in the complex with the azobenzene derivative **1**, which is due to van der Waals attraction between the exposed benzene ring of the ligand and the Pro1123 side chain (Figure S2). The side chain of Asp1124 is involved in a favorable polar interaction with the hydroxyl of Tyr1167 in all structures except for the complex with compound **1**.

Six of the 20 ligands (viz., compounds **3**, **11**−**14**, and **20**) have an amide linker which is involved in water-bridged interactions with the backbone carbonyl of Gln1113 (**3**, **12**−

DOI: 10.1021/acsmedchemlett.8b00286
ACS Med. Chem. Lett. 2018, 9, 929−934

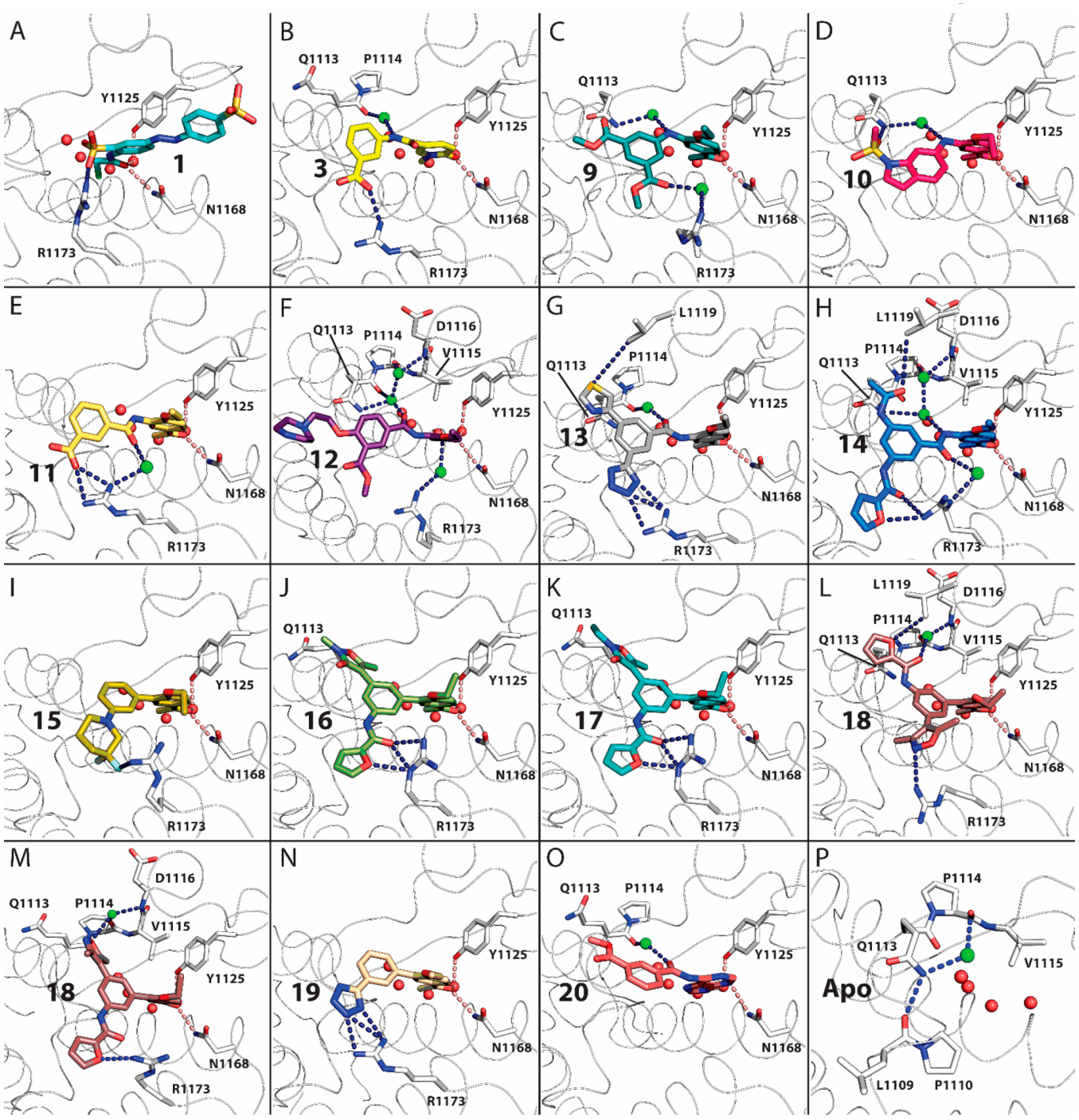

Figure 2. Interactions between the CBP bromodomain and small-molecule ligands. The spheres represent four conserved water molecules (red) and other water molecules involved in ligand binding (green). Conserved hydrogen bonds with the side chains of Asn1168 and Tyr1125 are shown (dashed lines in salmon). Other interactions between ligands and CBP bromodomain are emphasized (dashed lines in blue). (M) Ligand **18** shows alternate binding modes in different protein molecules in the asymmetric unit. (P) The conformation of Gln1113 is stabilized by hydrogen bonding interactions in the apo crystal structure of CBP bromodomain (PDB ID 3DWY).

14, and **20**) and/or the side chain of Arg1173 (**11** and **14**). The direct comparison of the amide linkers in compounds **3** and **20**, which point in opposite directions in the 2D structures, shows that the same water-bridged interaction with the backbone carbonyl of Gln1113 can be formed with a donor -NH- or acceptor -CO- (Figure 2B and O). Ligands **9** and **10** have a -NH_2- linker which is involved in water-bridged hydrogen bond interactions with the backbone carbonyl of Gln1113 similar to the amide linker containing ligands.

It is interesting to analyze the influence of the linker in the 12 acetyl-benzene derivatives (compounds **8**−**19**). A comparison of compounds **13** and **19** shows that the difference between direct covalent bond and amide linker does not influence the orientation of the tetrazole tail group which makes in both cases an ionic interaction with the side chain of Arg1173 (Figure 2G and 2N). The amide linker in ligands **11** and **14** shows opposite orientation as compared to that of the ligands **12** and **13**, thereby influencing the position of the

DOI: 10.1021/acsmedchemlett.8b00286
ACS Med. Chem. Lett. 2018, 9, 929−934

benzene ring (Figure 2 and S3A). Concerning the -NH_2- linker, the overlap of compounds **9** and the amide-linked **12** indicates that there is a substantial difference in the orientation of the benzene ring and the methyl ester in the meta position of the tail group (Figure S3B).

The purine ring in compound **20** shows a similar binding mode to the conserved asparagine (Asn1168 in CBP bromodomain) and tyrosine (Tyr1125 in CBP bromodomain) as the 2-amine-9H-purine containing ligand **7d** in the bromodomain of BRD9 (Figure S4A and S4B).[19] The mercaptopurine compound **4** binds to the BRPF1 bromodomain in a different way as the carbonyl group on the purine ring forms a bifurcated hydrogen bond with the conserved asparagine and tyrosine (Asn708 and Tyr665 in BRPF1 bromodomain, respectively) (Figure S4C).[20] The orientation of the purine scaffold in these three compounds is influenced by the size of the so-called "gatekeeper" residue (Val1174, Tyr106, and Phe714 in CBP, BRD9, and BRPF1 bromodomain, respectively) (Figure S4D), which is consistent with a previous report.[21]

We do not discuss the structure−activity relationship in detail for the 20 compounds because of their heterogeneity. Concerning the series of 12 derivatives of acetylbenzene (compounds **8** to **19**), it emerges that low nM affinity can be reached by engaging Arg1173 via a salt bridge (compounds **13** and **19**) or charge-dipole(s) interactions (compounds **14** and **18**). The linker does not contribute directly to the binding energy as compounds **13** and **14** have an amide linker while compounds **18** and **19** feature a single covalent bond between the head and tail groups. The linker does contribute to the selectivity as the acetylbenzene derivatives with the amide linker are more selective against the N-terminal domain of BRD4 (BRD4(1)) because their tail group clashes into the Trp81 side chain of BRD4(1).[12]

CONCLUSIONS

We have analyzed the binding motifs of 20 ligands of the CBP bromodomain. Nine of these ligands are docking hits[9,21,22] while the remaining ligands (compounds **9**−**19**) were synthesized in an optimization campaign.[12] Most of these ligands have favorable ligand efficiency (LE > 0.30 kcal/(mol HA)) irrespective of their size (Table 1). The conserved hydrogen bond with the NH_2 of Asn1168 is observed for the 20 ligands similarly to the hydrogen bond formed by the natural ligand acetyl-lysine.

Three new observations emerge from the analysis of the structural alignment. First, the interactions with the rim of the binding site are very heterogeneous. The variability in these interactions is congruent with the chemical diversity of the tail groups and flexibility of the ZA loop as observed in crystal structures and molecular dynamics simulations.[23−28] Compared to the apo structure, the ZA loop is slightly displaced toward the BC loop to optimize the van der Waals contacts with the ligands.

Second, there are multiple water-bridged interactions, and some rarely observed interaction types. The latter include a charge−dipole interaction between -CF_2- on ligand **15** and guanidinium of Arg1173, halogen−aromatic interaction between the chlorine of ligand **1** and phenyl of Phe1111, and aromatic−amide packing of the thiazole of compound **13** and the side chain of Gln1113.

Third, the 12 compounds that share an acetyl-benzene moiety as head can be clustered in three different groups according to the linker that connects the head and tail groups. The binding modes of the compounds with the amide linker are more similar to the poses of the compounds with a direct covalent bond than the derivatives with an amino linker. Thus, the relative orientation of head and tail groups has a stronger influence on the binding mode than their distance.

All crystal structures have been released in the PDB which should facilitate the structure-based optimization of CBP ligands.

ASSOCIATED CONTENT

Supporting Information

The Supporting Information is available free of charge on the ACS Publications website at DOI: 10.1021/acsmedchemlett.8b00286.

Experimental methods, X-ray crystal structure statistics data, electron density maps of bound ligands, characterization data of all synthesized compounds, structural analyses of all reported crystal structures, and dose−response curves for both BROMOscan and AlphaScreen assays (PDF)

Molecular formula strings for ligands **1** to **20** (XLSX)

Accession Codes

PDB accession codes of the structures of the CBP bromodomain in complex with small molecules are **1**(5EIC), **2**(5OWK), **3**(5EP7), **9**(5MME), **10**(5MMG), **12**(5ENG), **13**(5MPK), **15**(6FQU), **16**(6FQO), **17**(6FR0), **18**(6FRF), **19**(5MPN), and **20**(5H85). Authors will release the atomic coordinates and experimental data upon article publication.

AUTHOR INFORMATION

Corresponding Authors

*Phone: +41 44 635 55 21. E-mail: caflisch@bioc.uzh.ch.
*Phone: +41 44 635 39 45. E-mail: cristina.nevado@chem.uzh.ch.

ORCID

Jian Zhu: 0000-0002-2486-3658
Cristina Nevado: 0000-0002-3297-581X
Amedeo Caflisch: 0000-0002-2317-6792

Funding

We acknowledge financial support from the Swiss National Science Foundation (to A.C.), the Sinergia program (to C.N. and A.C.), the Synapsis Foundation-Alzheimer Research Switzerland, and the Heidi Seiler-Stiftung (to A.C., C.N., and P.S.).

Notes

The authors declare no competing financial interest.

ACKNOWLEDGMENTS

We thank the staff at X06DA and X06SA beamlines, Swiss Light Source, Paul Scherrer Institute (Villigen, Switzerland) for assistance in data collection.

ABBREVIATIONS

Alpha, amplified luminescent proximity homogeneous assay; BRD4, bromodomain 4; BRD9, bromodomain 9; BRPF1, Bromodomain and PHD Finger Containing Protein 1; CBP, CREB Binding Protein; CREB, cyclic-AMP response element binding protein.

DOI: 10.1021/acsmedchemlett.8b00286
ACS Med. Chem. Lett. 2018, 9, 929−934

REFERENCES

(1) Dhalluin, C.; Carlson, J. E.; Zeng, L.; He, C.; Aggarwal, A. K.; Zhou, M. M. Structure and ligand of a histone acetyltransferase bromodomain. *Nature* **1999**, *399* (6735), 491−6.

(2) Flynn, E. M.; Huang, O. W.; Poy, F.; Oppikofer, M.; Bellon, S. F.; Tang, Y.; Cochran, A. G. A Subset of Human Bromodomains Recognizes Butyryllysine and Crotonyllysine Histone Peptide Modifications. *Structure* **2015**, *23* (10), 1801−1814.

(3) Iyer, N. G.; Ozdag, H.; Caldas, C. p300/CBP and cancer. *Oncogene* **2004**, *23* (24), 4225−31.

(4) Mujtaba, S.; He, Y.; Zeng, L.; Yan, S.; Plotnikova, O.; Sachchidanand; Sanchez, R.; Zeleznik-Le, N. J.; Ronai, Z.; Zhou, M. M. Structural mechanism of the bromodomain of the coactivator CBP in p53 transcriptional activation. *Mol. Cell* **2004**, *13* (2), 251−63.

(5) Hay, D. A.; Fedorov, O.; Martin, S.; Singleton, D. C.; Tallant, C.; Wells, C.; Picaud, S.; Philpott, M.; Monteiro, O. P.; Rogers, C. M.; Conway, S. J.; Rooney, T. P.; Tumber, A.; Yapp, C.; Filippakopoulos, P.; Bunnage, M. E.; Muller, S.; Knapp, S.; Schofield, C. J.; Brennan, P. E. Discovery and optimization of small-molecule ligands for the CBP/p300 bromodomains. *J. Am. Chem. Soc.* **2014**, *136* (26), 9308−19.

(6) Rooney, T. P.; Filippakopoulos, P.; Fedorov, O.; Picaud, S.; Cortopassi, W. A.; Hay, D. A.; Martin, S.; Tumber, A.; Rogers, C. M.; Philpott, M.; Wang, M.; Thompson, A. L.; Heightman, T. D.; Pryde, D. C.; Cook, A.; Paton, R. S.; Muller, S.; Knapp, S.; Brennan, P. E.; Conway, S. J. A series of potent CREBBP bromodomain ligands reveals an induced-fit pocket stabilized by a cation-pi interaction. *Angew. Chem., Int. Ed.* **2014**, *53* (24), 6126−30.

(7) Crawford, T. D.; Romero, F. A.; Lai, K. W.; Tsui, V.; Taylor, A. M.; de Leon Boenig, G.; Noland, C. L.; Murray, J.; Ly, J.; Choo, E. F.; Hunsaker, T. L.; Chan, E. W.; Merchant, M.; Kharbanda, S.; Gascoigne, K. E.; Kaufman, S.; Beresini, M. H.; Liao, J.; Liu, W.; Chen, K. X.; Chen, Z.; Conery, A. R.; Cote, A.; Jayaram, H.; Jiang, Y.; Kiefer, J. R.; Kleinheinz, T.; Li, Y.; Maher, J.; Pardo, E.; Poy, F.; Spillane, K. L.; Wang, F.; Wang, J.; Wei, X.; Xu, Z.; Xu, Z.; Yen, I.; Zawadzke, L.; Zhu, X.; Bellon, S.; Cummings, R.; Cochran, A. G.; Albrecht, B. K.; Magnuson, S. Discovery of a Potent and Selective in Vivo Probe (GNE-272) for the Bromodomains of CBP/EP300. *J. Med. Chem.* **2016**, *59* (23), 10549−10563.

(8) Xu, M.; Unzue, A.; Dong, J.; Spiliotopoulos, D.; Nevado, C.; Caflisch, A. Discovery of CREBBP Bromodomain Inhibitors by High-Throughput Docking and Hit Optimization Guided by Molecular Dynamics. *J. Med. Chem.* **2016**, *59* (4), 1340−9.

(9) Spiliotopoulos, D.; Zhu, J.; Wamhoff, E. C.; Deerain, N.; Marchand, J. R.; Aretz, J.; Rademacher, C.; Caflisch, A. Virtual screen to NMR (VS2NMR): Discovery of fragment hits for the CBP bromodomain. *Bioorg. Med. Chem. Lett.* **2017**, *27* (11), 2472−2478.

(10) Romero, F. A.; Murray, J.; Lai, K. W.; Tsui, V.; Albrecht, B. K.; An, L.; Beresini, M. H.; de Leon Boenig, G.; Bronner, S. M.; Chan, E. W.; Chen, K. X.; Chen, Z.; Choo, E. F.; Clagg, K.; Clark, K.; Crawford, T. D.; Cyr, P.; de Almeida Nagata, D.; Gascoigne, K. E.; Grogan, J. L.; Hatzivassiliou, G.; Huang, W.; Hunsaker, T. L.; Kaufman, S.; Koenig, S. G.; Li, R.; Li, Y.; Liang, X.; Liao, J.; Liu, W.; Ly, J.; Maher, J.; Masui, C.; Merchant, M.; Ran, Y.; Taylor, A. M.; Wai, J.; Wang, F.; Wei, X.; Yu, D.; Zhu, B. Y.; Zhu, X.; Magnuson, S. GNE-781, A Highly Advanced Potent and Selective Bromodomain Inhibitor of Cyclic Adenosine Monophosphate Response Element Binding Protein, Binding Protein (CBP). *J. Med. Chem.* **2017**, *60* (22), 9162−9183.

(11) Unzue, A.; Xu, M.; Dong, J.; Wiedmer, L.; Spiliotopoulos, D.; Caflisch, A.; Nevado, C. Fragment-Based Design of Selective Nanomolar Ligands of the CREBBP Bromodomain. *J. Med. Chem.* **2016**, *59* (4), 1350−6.

(12) Batiste, L.; Unzue, A.; Dolbois, A.; Hassler, F.; Wang, X.; Deerain, N.; Zhu, J.; Spiliotopoulos, D.; Nevado, C.; Caflisch, A. Chemical Space Expansion of Bromodomain Ligands Guided by in Silico Virtual Couplings (AutoCouple). *ACS Cent. Sci.* **2018**, *4* (2), 180−188.

(13) Xiang, Q.; Wang, C.; Zhang, Y.; Xue, X.; Song, M.; Zhang, C.; Li, C.; Wu, C.; Li, K.; Hui, X.; Zhou, Y.; Smaill, J. B.; Patterson, A. V.; Wu, D.; Ding, K.; Xu, Y. Discovery and optimization of 1-(1H-indol-1-yl)ethanone derivatives as CBP/EP300 bromodomain inhibitors for the treatment of castration-resistant prostate cancer. *Eur. J. Med. Chem.* **2018**, *147*, 238−252.

(14) Philpott, M.; Yang, J.; Tumber, T.; Fedorov, O.; Uttarkar, S.; Filippakopoulos, P.; Picaud, S.; Keates, T.; Felletar, I.; Ciulli, A.; Knapp, S.; Heightman, T. D. Bromodomain-peptide displacement assays for interactome mapping and inhibitor discovery. *Mol. BioSyst.* **2011**, *7* (10), 2899−908.

(15) Hopkins, A. L.; Keseru, G. M.; Leeson, P. D.; Rees, D. C.; Reynolds, C. H. The role of ligand efficiency metrics in drug discovery. *Nat. Rev. Drug Discovery* **2014**, *13* (2), 105−21.

(16) Zhang, G.; Smith, S. G.; Zhou, M. M. Discovery of Chemical Inhibitors of Human Bromodomains. *Chem. Rev.* **2015**, *115* (21), 11625−68.

(17) Filippakopoulos, P.; Knapp, S. Targeting bromodomains: epigenetic readers of lysine acetylation. *Nat. Rev. Drug Discovery* **2014**, *13* (5), 337−56.

(18) Bamborough, P.; Chung, C. W.; Demont, E. H.; Furze, R. C.; Bannister, A. J.; Che, K. H.; Diallo, H.; Douault, C.; Grandi, P.; Kouzarides, T.; Michon, A. M.; Mitchell, D. J.; Prinjha, R. K.; Rau, C.; Robson, S.; Sheppard, R. J.; Upton, R.; Watson, R. J. A Chemical Probe for the ATAD2 Bromodomain. *Angew. Chem., Int. Ed.* **2016**, *55* (38), 11382−6.

(19) Picaud, S.; Strocchia, M.; Terracciano, S.; Lauro, G.; Mendez, J.; Daniels, D. L.; Riccio, R.; Bifulco, G.; Bruno, I.; Filippakopoulos, P. 9H-purine scaffold reveals induced-fit pocket plasticity of the BRD9 bromodomain. *J. Med. Chem.* **2015**, *58* (6), 2718−36.

(20) Zhu, J.; Caflisch, A. Twenty Crystal Structures of Bromodomain and PHD Finger Containing Protein 1 (BRPF1)/Ligand Complexes Reveal Conserved Binding Motifs and Rare Interactions. *J. Med. Chem.* **2016**, *59* (11), 5555−61.

(21) Unzue, A.; Zhao, H.; Lolli, G.; Dong, J.; Zhu, J.; Zechner, M.; Dolbois, A.; Caflisch, A.; Nevado, C. The ″Gatekeeper″ Residue Influences the Mode of Binding of Acetyl Indoles to Bromodomains. *J. Med. Chem.* **2016**, *59* (7), 3087−97.

(22) Spiliotopoulos, D.; Wamhoff, E. C.; Lolli, G.; Rademacher, C.; Caflisch, A. Discovery of BAZ2A bromodomain ligands. *Eur. J. Med. Chem.* **2017**, *139*, 564−572.

(23) Filippakopoulos, P.; Picaud, S.; Mangos, M.; Keates, T.; Lambert, J. P.; Barsyte-Lovejoy, D.; Felletar, I.; Volkmer, R.; Muller, S.; Pawson, T.; Gingras, A. C.; Arrowsmith, C. H.; Knapp, S. Histone recognition and large-scale structural analysis of the human bromodomain family. *Cell* **2012**, *149* (1), 214−31.

(24) Marchand, J. R.; Caflisch, A. Binding Mode of Acetylated Histones to Bromodomains: Variations on a Common Motif. *ChemMedChem* **2015**, *10* (8), 1327−33.

(25) Langini, C.; Caflisch, A.; Vitalis, A. The ATAD2 bromodomain binds different acetylation marks on the histone H4 in similar fuzzy complexes. *J. Biol. Chem.* **2017**, *292* (40), 16734−16745.

(26) Magno, A.; Steiner, S.; Caflisch, A. Mechanism and Kinetics of Acetyl-Lysine Binding to Bromodomains. *J. Chem. Theory Comput.* **2013**, *9* (9), 4225−32.

(27) Steiner, S.; Magno, A.; Huang, D.; Caflisch, A. Does bromodomain flexibility influence histone recognition? *FEBS Lett.* **2013**, *587* (14), 2158−63.

(28) Zhu, J.; Zhou, C.; Caflisch, A. Structure-based discovery of selective BRPF1 bromodomain inhibitors. *Eur. J. Med. Chem.* **2018**, *155*, 337−352.

DOI: 10.1021/acsmedchemlett.8b00286
ACS Med. Chem. Lett. 2018, 9, 929−934